Effect of ultrasound pretreatment on bromination of double-walled carbon nanotubes

L.G. Bulusheva[a,b,*], E.V. Lobiak[a], Yu.V. Fedoseeva[a], J.-Y. Mevellec[c], A.A. Makarova[d], E. Flahaut[e], A.V. Okotrub[a,b]

[a] Nikolaev Institute of Inorganic Chemistry, SB RAS, 3 Acad. Lavrentiev Ave., 630090 Novosibirsk, Russia
[b] Tomsk State University, 36 Lenin Ave., 634050 Tomsk, Russia
[c] Institut des Matériaux Jean Rouxel, CNRS-Université de Nantes, UMR6502, 2 Rue de la Houssinière, BP32229, 44322 Nantes Cedex 3, France
[d] Physical Chemistry, Institute of Chemistry and Biochemistry, Free University of Berlin, Arnimallee 22, 14195 Berlin, Germany
[e] CIRIMAT, Université de Toulouse, CNRS, INPT, UPS, UMR CNRS-UPS-INP N°5085, Université Toulouse 3 Paul Sabatier, Bât. CIRIMAT, 118, route de Narbonne, 31062 Toulouse cedex 9, France

ABSTRACT

Bromination of double-walled carbon nanotubes (DWCNTs) was carried out using a saturated vapor of Br_2 at room temperature with or without a pretreatment in bromine water. X-ray photoelectron spectroscopy revealed that ultrasound pretreatment modified the chemical state of bromine in the product. The binding energies of the Br 3d electrons in the pre-sonicated DWCNT sample were between those characteristic of the covalent C–Br bonds and the negatively charged Br_2 molecules, observed when the pretreatment was not performed. Raman spectroscopy, however, clearly evidenced Br–Br vibrations in both brominated samples. Calculations of CNT–Br_2 models within density functional theory were used to propose that the electronic state of a Br_2 molecule depends on the adsorption site. The bromine molecules prefer to be located near edge hydroxyl groups, which acept the electron density from Br_2. This increases the binding energy of Br 3d levels as compared to that for Br_2 molecules in other adsorption sites.

1. Introduction

Bromination is a way to change the electronic structure and chemical reactivity of carbon materials. Graphite intercalation compounds with bromine have long been known [1]. The guest Br_2 molecules accept electron density from graphene planes [2], changing the electrical properties of the material. It has been demonstrated that bromine intercalation substantially increased the conductivity of few layer graphene [3]. Similarly, it has also been shown that the treatment of graphitic materials by liquid or gaseous Br_2 improved their electrochemical properties in Li ion cells [4,5]. Bromine can also form covalent bonds with carbon atoms. Such bonds are preferably organized when bromine plasma is used during the synthesis [6,7]. Covalent C Br bonds can further participate in nucleophilic substitution reactions for grafting of desired functionalities to a carbon skeleton [6,8,9].

Single walled and double walled carbon nanotubes (SWCNTs and DWCNTs) are usually gathered into ropes and bromine can intercalate into intertube space, or adsorb on the nanotubes composing the rope surface. Density functional theory (DFT) calculations have shown that

Br_2 molecules are weakly bonded with a SWCNT surface and unoccupied bromine states form a band above the Fermi level of the nanotube [10]. These states overlap with carbon bands when Br_2 molecules are intercalated into SWCNT ropes [11]. In practice, bromination can assist in the purification of CNTs from the synthesis by products [12] and the separation of metallic and semiconducting SWCNTs [13]. The use of bromine functionalized SWCNTs as efficient gas chemiresistor sensors [14] has also been demonstrated.

A study of brominated graphite nanoplatelets has revealed that the electrical conductivity is improved by ionically bonded bromine, whereas the opposite was observed with covalently bonded bromine [15]. The same trend was observed for the conductivity of multi walled CNTs (MWCNTs) after covalent [16] and ionic [17] bromine functionalization. Since the electronic properties of brominated carbon depend on the C Br interaction, it is important to identify its character. The most suitable method to achieve this is X ray photoelectron spectroscopy (XPS) [18]. The XPS Br 3d spectrum of microwave assisted brominated DWCNTs exhibited a single doublet with a Br $3d_{5/2}$ component at 70 eV, which was unambiguously assigned to the covalent C Br

bonding [19]. The component at 68.5 ± 0.2 eV was attributed to the adsorbed Br_2 molecules, because its intensity was substantially suppressed after sample annealing [20]. Raman spectroscopy was used to elucidate the charge of the intercalated/adsorbed Br_2 [21]. The Raman active Br Br stretching mode at 323 cm ^{1} for the gaseous Br_2 molecules shifts to 242 cm ^{1} in the intercalated graphite bromine system. The intramolecular interactions and charge transfer between the host matrix and intercalants define this Raman shift and using temperature dependent Raman spectra, the charge transfer was roughly estimated to be 0.34e per Br_2 [22].

DWCNTs are particularly interesting for the functionalization because the outer nanotubes protect the inner ones. Studies of the Raman spectra of the DWCNTs treated with Br_2 vapors have revealed a drop in the intensities of radial breathing modes (RBM) from the outer nanotubes and little changes for the inner nanotubes, when they were metallic [23,24]. This is due to a strong sensitivity of metallic nanotubes to chemical doping. The outer metallic nanotube screens the inner semiconducting nanotube from the external environment [25].

In this paper, using information obtained from XPS and Raman spectroscopy, we show that the interaction of Br_2 with graphitic carbon may depend on the presence of surface oxygen containing groups. This result is obtained from the comparison between two DWCNT samples brominated using a saturated Br_2 vapor at room temperature. One starting sample was DWCNTs purified from carbon co products by heating in air at 550 °C. The other starting sample was prepared using an ultrasound treatment of the brominated purified DWCNTs in bromine water with the purpose to increase the content of grafted oxygen containing groups. It was shown previously that the brominated CNTs are more easily oxidized than those without bromination [26]. Interpretation of the experimental data is supported by DFT calculations.

2. Materials and methods

2.1. Materials

DWCNTs were synthesized by the catalytic chemical vapor deposition (CCVD) method using a catalyst with a target composition of $MgO_{0.99}(Co_{1\ x}Mo_x)_{0.01}O$ with x = 0.25 and a mixture of CH_4 and H_2 gases at 1000 °C [27]. The product was treated by a concentrated aqueous HCl solution to remove the MgO support as well as all the accessible metals. The obtained powder material is a mixture of disorganized carbon, which is deposited on the catalyst free MgO surface [28], and CNTs with a number of walls ranging from one to three. High resolution transmission electron microscopy (HRTEM) study has revealed that typical samples contain *ca.* 80 % of DWCNTs with a mean outer diameter of 2.05 nm [27]. To remove the disorganized carbon, the powder was heated in air at 550 °C for 30 min followed by washing with a concentrated aqueous HCl solution. The obtained suspension was filtered over a cellulose nitrate membrane and the DWCNTs were washed by deionized water until neutral pH before freeze drying.

The purified DWCNTs (0.02 g) were put in a perforated Teflon flask which was placed on a stand in a larger Teflon flask containing liquid bromine (2 mL) at the bottom. The sample was held at room temperature in saturated bromine vapors for two days. The product was flushed by a flow of N_2 to remove weakly bonded Br_2. The sample is referred as **Br-DWCNTs**. This sample was treated using a pulsed ultrasound with a power of 450 W in bromine water for 30 min. Then, the suspension was filtered, the solid was dried in air and finally brominated using the above described procedure. The obtained sample is further denoted as **Br-usDWCNTs.**

2.2. Instrumentation

TEM characterization of the samples was carried out on a Jeol 2010 microscope operated at 200 kV. Raman spectra were measured using a Renishaw Invia spectrometer at 514.5 nm (2.41 eV, Ar^{+} laser) and 785.0 nm (1.58 eV, solid state laser) wavelengths.

XPS and near edge X ray absorption fine structure (NEXAFS) experiments were performed at the Berliner Elektronenspeicherring für Synchrotronstrahlung (BESSY II), Helmholtz Zentrum Berlin using the Russian-German beamline of monochromatized synchrotron radiation. NEXAFS spectra near the C K edge were acquired in the total electron yield mode and normalized to the primary photon current from a gold covered grid recorded simultaneously. The monochromatization of the incident radiation was ~80 meV (full width at half maximum, FWHM). The energy calibration was performed relative to the graphitic π* resonance at 285.4 eV. The overall XPS spectra, as well as the C 1s and Br 3d lines, were measured using monochromatized radiation energy of 830 eV with an energy resolution better than 0.4 eV, FWHM. The content of elements was evaluated from the ratio of the area under the corresponding core level peaks taking into consideration the photoionization cross sections at the given photon energy and transmission function of the analyzer. The background signal was subtracted by Shirley's method.

2.3. DFT calculations

A hybrid method MPWB1K based on the modified Perdew and Wang exchange functional and Becke's 1995 correlation functional [29] with the D3 correction developed by Grimme *et al.* for the dispersion interactions accounting [30] was used for the calculations within the program package Jaguar (Jaguar, version 10.3, Schrödinger, Inc., New York, NY, 2019). Atomic orbitals were presented by an STO 3 G basis set. Optimization of the geometry of Br_2 molecule at the MPWB1K D3/ STO 3 G level gave a bond length of 2.297 Å, which well agrees with the experimental value of 2.289 Å for gas phase Br_2 [31].

An outer DWCNT wall was modeled by a fragment of armchair (9,9) CNT with a length of *ca.* 22.2 Å, where the edges were terminated by hydrogen and oxygen containing groups. The diameter of this CNT is 12.3 Å and this value is minimal for the outer shells of the studied DWCNTs as determined from the HRTEM analysis [27]. Geometry optimizations were performed with default convergence criteria. The absence of imaginary frequencies indicated that the obtained structures corresponded to the local minima on potential energy surfaces.

3. Results and discussion

Comparative study of the obtained brominated samples by TEM did not reveal obvious differences between them (Fig. 1). It was previously shown that ultrasonication of bromine intercalated graphite in water results in splitting of graphite plates and in plane destruction of crystallites [32,33]. Although the images taken with a low magnification show that the nanotubes are more dispersed in the Br usDWCNTs sample (Fig. 1a, b), we cannot conclude unambiguously that the used ultrasonic treatment assists in debundling of the DWCNTs because the TEM is a very local method. Actually, the HRTEM images evidenced the presence of individual DWCNTs and small size bundles in both samples (Fig. 1c, d). It seems that surfaces of the sonicated DWCNTs are more contaminated by carbon deposits (Fig. 1d). This could indicate a larger number of defects in these nanotubes. Previous studies of multi walled CNTs after an ultrasound treatment in methylene chloride have shown buckling, bending and dislocations in the carbon structures [34]. Damaging of the nanotubes depended on the solvent, and was less visible when using water.

The content of bromine determined from the survey XPS spectra was *ca.* 1.8 at.% in Br DWCNTs and *ca.* 1.6 at.% in Br usDWCNTs. These values are very close, indicating that the used ultrasound pretreatment of DWCNTs in bromine water did not improve their reactivity towards gaseous Br_2. The oxygen content however increased from *ca.* 2.4 at.% in Br DWCNTs to *ca.* 3.6 at.% in Br usDWCNTs as the survey XPS spectra showed. Previously it has been observed that sonication assisted the oxidation of SWCNTs in a dilute aqueous ozone solution [35] and
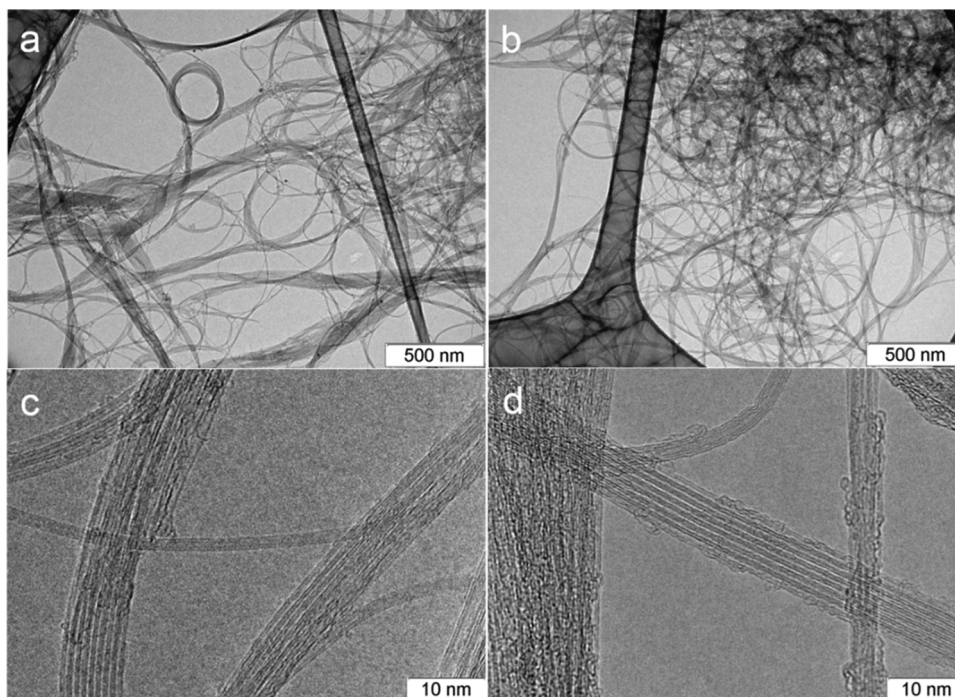
Fig. 1. Low-magnification (a, b) and high-magnification (c, d) TEM images of Br-DWCNTs (a, c) and Br-usDWCNTs (b, d).

MWCNTs in deionized water [36].

Electronic state of carbon in the samples was studied using XPS and NEXAFS spectroscopy. The XPS C 1s spectrum of initial purified DWCNTs exhibited an asymmetric peak at 284.5 eV (Fig. 2a) char acteristic of graphitic carbon [37]. The similarity of the spectral shape of these DWCNTs and Br DWCNTs corresponds to no noticeable mod ification of the electronic structure of the DWCNTs after their treatment by gaseous Br_2 at room temperature. Earlier, a study of a brominated DWCNT sample containing ~5.6 at.% bromine has shown a downshift of the C 1s line by ~0.4 eV as compared to the spectrum of non modified DWCNTs [20]. This shift was attributed to *p* doping of na notubes as the result of their interaction with adsorbed Br_2 molecules. It is likely that in the present case the amount of bromine on the surface of sample is not enough to detect the shift of C 1s line. However, NEXAFS spectroscopy was used to reveal the difference between empty C 2p electronic states of DWCNTs and Br DWCNTs (Fig. 2b). The NEXAFS C K edge spectrum of the latter sample exhibited a shoulder (labeled "A")

at the low energy side of π* resonance (Fig. 2b), which is attributed to charge transfer from carbon cages to bromine [38,39].

As compared to DWCNTs and Br DWCNTs, the XPS C 1s spectrum of Br usDWCNTs broadened by ~0.3 eV at half height (Fig. 2a), eviden cing that the applied sonication and bromination procedures modified the electronic structure of the nanotubes. This is reflected in the NEXAFS C K edge spectrum of Br usDWCNTs, which exhibited an in crease in the intensity at 288.5 eV and a suppression of the π* re sonance (Fig. 2b). The peak at 288.5 eV could be attributed to C O [40], C Br [41], and C H [42] bonds as well as amorphous carbon [7], a possible product of DWCNTs damages.

The nature of the oxygen containing groups present on the DWCNTs surface after the ultra sound treatment was evaluated from the fitting of XPS C 1s spectrum of Br usDWCNTs (Fig. 2a). Weak components at ~286.1 and ~288.8 eV correspond to carbon bonded to oxygen in hydroxyl group (−OH) and carbon from carboxyl group (−COOH), respectively [43]. The component at 285.2 eV can be attributed to
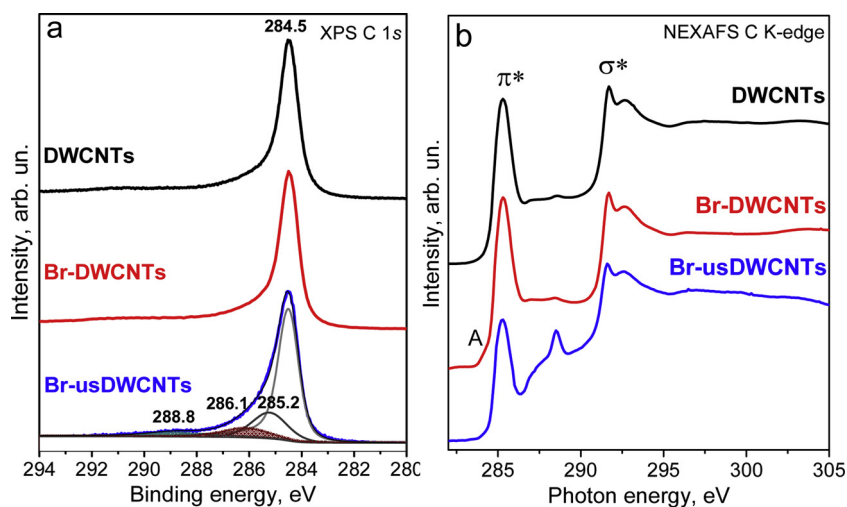

Fig. 2. XPS C 1s spectra (a) and NEXAFS C K-edge spectra (b) of initial DWCNTs, Br-DWCNTs, and Br-usDWCNTs.
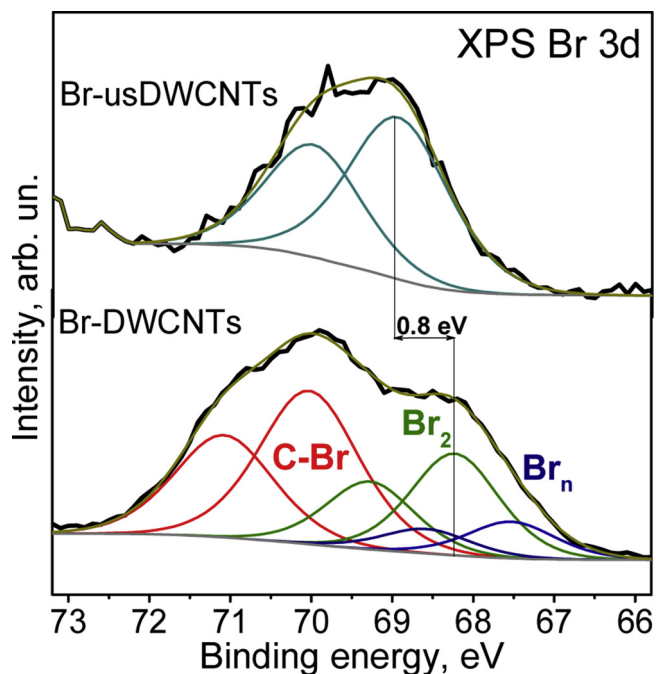
Fig. 3. XPS Br 3d spectra of Br-DWCNTs and Br-usDWCNTs.

various defects in CNTs [44].

Chemical states of bromine in the brominated samples were ob tained using XPS Br 3d spectra. Three spin orbit doublets fitted the spectrum of Br DWCNTs, while only one doublet was used in case of the Br usDWCNT spectrum (Fig. 3). Assignment of the components found in the latter spectrum was done using data available from the literature [18 20]. The Br $3d_{5/2}$ component at ~ 70.0 eV corresponds to covalent C Br bonds, which can develop at the DWCNT edges. The Br $3d_{5/2}$ component at ~ 68.2 eV is attributed to adsorbed Br_2 molecules and the low energy component at ~ 67.5 eV is due to polybromine species, which readily accept the electronic density from a graphene surface [44]. The Br $3d_{5/2}$ component in the spectrum of Br usDWCNTs is lo cated at ~ 69.0 eV, between the components from covalent C Br bonds and adsorbed Br_2 molecules.

Raman spectroscopy is a method for studying the interaction of DWCNTs with bromine. We used two excitation sources with energies of 1.58 eV (785.0 nm) and 2.41 eV (514.5 nm) to probe the combina tions of semiconducting inner and metallic outer nanotubes (S@M) and metallic inner and semiconducting outer (M@S) nanotubes, respec tively [24]. The data were acquired in three different places of a sample and Fig. 4 shows averaged spectra.

Fig. 4a compares the Raman spectra measured at 785.0 nm. The spectrum of starting DWCNTs exhibits a broad tangential G band

composed of a sharp peak at *ca.* 1589 cm ^{1} coming from the vibrations from inner and outer nanotubes and a peak at *ca.* 1560 cm ^{1} related to electronic interwall interactions [46]. The disorder induced D band has a negligible intensity indicating a high purity of the DWCNT sample after heating of the CCVD product in air at 550 °C. The band slightly grows in the spectra of Br DWCNTs and Br usDWCNTs and this can be related to attachment of functional groups. An intense peak at 271 cm ^{1} as well as weaker peaks at 169, 160, and 150 cm ^{1} are observed in the RBM region. The latter peak is absent in the Raman spectra of the brominated DWCNTs. According to the Kataura plot, it corresponds to a metallic nanotube [47]. Moreover, G bands of brominated DWCNTs samples are broadened due to upshifts of the component assigned to the vibrations from outer nanotubes. Thus, we can conclude that Br_2 mo lecules interact with the outer metallic nanotubes. It seems that this interaction is stronger in the Br us DWCNTs, whose spectrum shows a larger broadening of the G band. Note that previous studies of the effect of bromination on Raman spectra of DWCNTs did not evidence such changes in the G band at an excitation of 785.0 nm [23]. Those DWCNTs were however produced by another technique, which is likely to yield much less outer metallic shells than in our case.

The Raman spectra measured for brominated DWCNTs at 514.5 nm did not show a noticeable broadening of the G band as compared to that of initial DWCNTs (Fig. 4b). In this case, semiconducting outer nano tubes dominate the G band. Their tangential vibrations increased slightly only by *ca.* 4 cm ^{1} in the spectrum of Br DWCNTs and *ca.* 2 cm ^{1} in that of Br usDWCNTs. Such small upshifts are due to a low bromine content in the samples [20]. The fact that upshift of the G band was not accompanied by the band broadening supposes that both metallic inner and semiconducting outer nanotubes sense the adsorbed bromine [23]. At this excitation energy, Br Br stretching vibrations are in resonance giving an intense peak at 232 cm ^{1}. Additionally, the Raman spectrum of brominated samples exhibited a peak at 153 cm ^{1}, attributed to polybromine Br_n chains [45,48]. Our recent calculations have shown the chains are mainly composed of the Br_3 based species [49]. Bromine related peaks overlap with RBMs from the outer nanotubes, which does not allow revealing changes in their electronic structure as the result of bromination. The RBM peaks located between 335 and 250 cm ^{1} are attributed to the inner nanotubes visible in the spectra of brominated samples. This confirms a weak interaction of the inner metallic nano tubes with bromine situated on external surfaces of DWCNTs.

Thus, Raman spectroscopy identified Br_2 molecules in Br DWCNTs as well as in Br usDWCNTs, whereas XPS found a difference in binding energies of Br 3d electrons in these samples. To understand the reason of this disagreement, we invoked the DFT calculations. The XPS data identified the increase in the oxygen content in Br usDWCNTs as $-OH$ and $-COOH$ groups (Fig. 2a). The emergence of these groups was ac companied by the disappearance of covalent C Br bonds, as the com parison of Br 3d spectra of Br DWCNTs and Br usDWCNTs illustrated. The C Br bonds were most likely on the DWCNT edges. They were
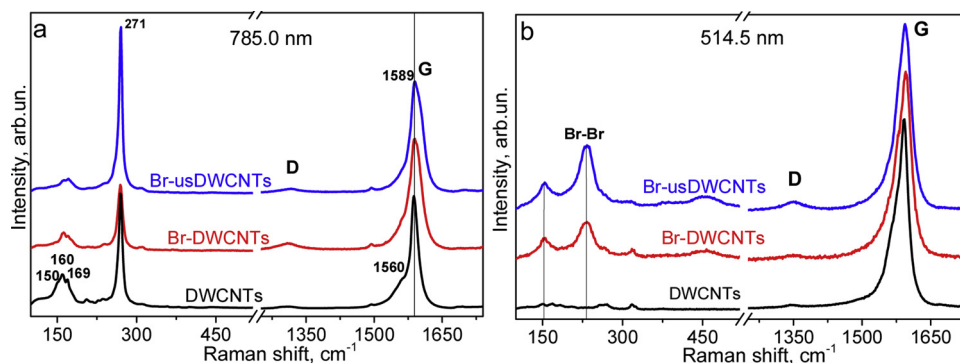

Fig. 4. Raman spectra of DWCNTs, Br-DWCNTs, and Br-usDWCNTs measured at excitation wavelengths of 785.0 nm (a) and 514.5 nm (b). The spectra were normalized to the intensity of G band.
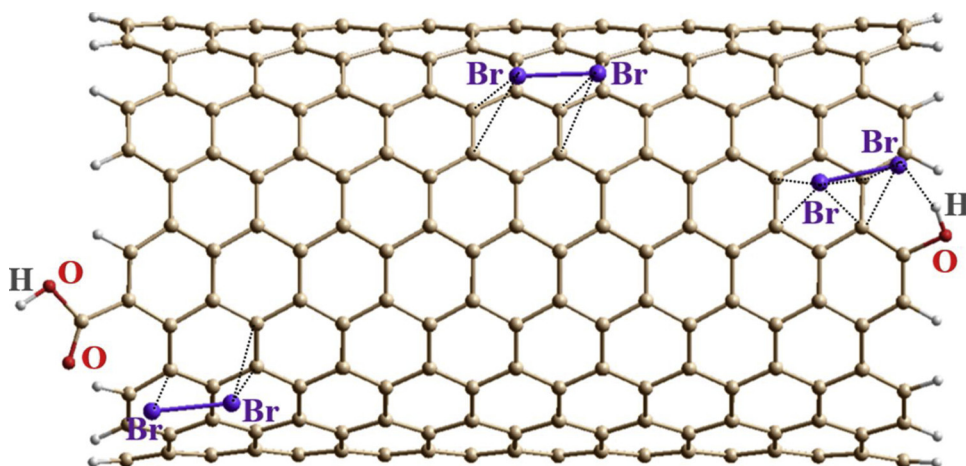
Fig. 5. Positions of Br_2 molecules at perfect nanotube surface (center) and near carboxyl group (left) and hydroxyl group (right). This structure was plotted using the results of geometry optimization for three considered CNT–Br_2 models. The distances between components less than 3.60 Å are shown by dotted lines.

Table 1

Energetic and structural data obtained from the MPWB1K-D3/STO-3 G calculation of three CNT–Br_2 models with different locations of Br_2. The total energies, charge, and Br 3d eigenvalues are given relative to the corresponding value for the model with center Br_2 location.

Br_2 location	ΔE_{tot} (eV)	ΔBr_2 charge	ΔBr 3d (eV)	Shortest C-Br distances (Å)
CNT center	0	0	0	3.55 – 3.58
near –COOH	+0.021	0	+0.12	3.57 – 3.59
near –OH	0.095	+0.04e	0.77	3.42 – 3.59

disrupted during the sonication procedure and the oxygen containing groups were developed instead of bromine. This correlates with literature observations [6].

In the modelling, −OH and −COOH groups were attached to the opposite ends of the CNT fragment (Fig. 5). Three CNT Br$_2$ models were considered where a Br_2 molecule was located near the hydroxyl group, near the carboxyl group or over the central part of the CNT fragment. The length of the fragment is large enough so that its edges should not affect markedly the state of the molecule, which was located at the center. Comparison of the total energies of the models after optimization procedures showed that the most stable Br_2 position is near the hydroxyl group (Table 1). The energy gain is due to the attractive interaction between a bromine atom of Br_2 and hydrogen atom of OH group. The distance between this bromine atom and hydrogen is about 2.39 Å. Moreover, the second bromine atom is located almost above the center of carbon hexagons that produces four Br C contacts shorter than 3.60 Å (Fig. 5, Table 1). Results of the optimization geometry of two other CNT Br$_2$ models showed that the Br_2 molecule closely contacted with four and three carbon atoms when it localized over the central CNT part, and near carboxyl group, respectively (Fig. 5). However, the energies of the models differ by no more than 0.116 eV (Table 1) and we conclude from this that all considered Br_2 sites are possible when the synthesis is carried out at room temperature.

Next, we examined the eigenvalues corresponding to core Br 3d levels of Br_2 adsorbates. The average absolute value is 50.6 eV for the Br_2 adsorbed at the perfect CNT surface and 50.48 eV for the Br_2 located near the carboxyl group. Hence, the energy resolution of the measured XPS spectra does not allow distinguishing between these two species. The absolute Br 3d eigenvalue for the Br_2 adsorbed at the hydroxyl group is 51.37 eV and this value is larger by 0.77 0.89 eV as compared to that calculated for other Br_2 adsorbates (Table 1). This difference between core level energies perfectly agrees with the experimental shift of 0.8 eV observed for Br usDWCNTs relative to the state of Br_2 in Br usDWCNTs (Fig. 3). Our calculations show that such a shift to higher binding energy is due to a positive charging of Br_2 molecule when it is near the hydroxyl group (Table 1). However, this change in the charge

transfer causes no change in the Br Br length as compared to that for Br_2 located at perfect CNT region, and this is the reason of the similarity of bromine related Raman scattering observed for Br DWCNTs and Br usDWCNTs samples (Fig. 4b).

4. Conclusions

Holding the purified DWCNT sample in saturated bromine vapors at room temperature for two days resulted in attachment of 1.8 at. % of bromine. About half of this amount was in the form of Br_2 while another part of bromine atoms formed covalent bonds with edge carbon atoms. Our results show that when the sample was first sonicated in bromine water, these C Br bonds were broken, and edge hydroxyl and carboxyl groups were formed instead. These groups keep the DWCNT edges free from bromine during the subsequent bromination of the sample after sonication. Raman spectroscopy evidenced that bromine in pre sonicated DWCNT sample was in the molecular Br_2 form. The interaction of the Br_2 molecules with outer metallic nanotubes was stronger than in the case of non sonicated sample. The XPS study detected the difference in binding energies of the adsorbed Br_2 species for two types of DWCNT samples. Br_2 molecules in the pre sonicated sample were charged positively as compared to those in the initial sample. The DFT calculations revealed that this charging is due to the electron withdrawing ability of hydroxyl groups located at the nanotube edges. These groups are attractive for Br_2 molecules and this fact may be used to develop a strategy for increasing the doping level of graphitic carbon *via* bromination.

Declaration of Competing Interest

The authors declare that they have no known competing financial interests or personal relationships that could have appeared to influence the work reported in this paper.

References

[1] W. Rüdorff, Uber die Lösung von Brom im Kristallgitter des Graphits, Bromgraphit, Z. Anorg. Allg. Chem. 245 (1940) 383–390.

[2] A. Yaya, C.P. Ewels, I. Suarez–Martinez, Ph. Wagner, S. Lefrant, A. Okotrub, L. Bulusheva, P.R. Briddon, Bromination of graphene and graphite, Phys. Rev. B 83 (2011) 045411.

[3] A.E. Mansour, S. Dey, A. Amassian, M.H. Tanielian, Bromination of graphene: a new

route to making high performance transparent conducting electrodes with low optical losses, ACS Appl. Mater. Interfaces 7 (2015) 17692–17699.

[4] P. Barpanda, G. Fanchinii, G.G. Amatucci, Structure, surface morphology and electrochemical properties of brominated activated carbons, Carbon 49 (2011) 2538–2548.

[5] V.O. Koroteev, W. Münchgesang, Yu.V. Shubin, Yu.N. Palyanov, P.E. Plyusnin, D.A. Smirnov, K.A. Kovalenko, M. Bobnar, R. Gumeniuk, E. Brendler, D.C. Meyer, L.G. Bulusheva, A.V. Okotrub, A. Vyalikh, Multiscale characterization of ^{13}C–enriched fine–grained graphitic materials for chemical and electrochemical applications, Carbon 124 (2017) 161–169.

[6] J.F. Friedrich, S. Wettmarshausen, S. Hanelt, R. March, R. Mix, E.B. Zeynalov, A. Meyer–Plath, Plasma–chemical bromination of graphitic materials and its use for subsequent functionalization and grafting of organic molecules, Carbon 48 (2010) 3884–3894.

[7] A. Lippitz, J.F. Friedrich, W.E.S. Unger, Plasma bromination of HOPG surfaces: a NEXAFS and synchrotron XPS study, Surf. Sci. 611 (2013) L1–L7.

[8] J. Zheng, H.–T. Liu, B. Wu, C.–A. Di, Y.–L. Guo, T. Wu, G. Yu, Y.–Q. Liu, D.–B. Zhu, Production of graphite chloride and bromide using microwave sparks, Sci. Rep. 2 (2012) 662.

[9] H. Au, N. Rubio, M.S.P. Shaffer, Brominated graphene as a versatile precursor for multifunctional grafting, Chem. Sci. 9 (2018) 209–217.

[10] N. Park, Y. Miyamoto, K. Lee, W.I. Choi, J. Ihm, J. Yu, S. Han, Band gap sensitivity of bromine adsorption at carbon nanotubes, Chem. Phys. Lett. 403 (2005) 135–139.

[11] S.–H. Jhi, S.G. Louie, M.L. Cohen, Electronic properties of bromine–doped carbon nanotubes, Solid State Commun. 123 (2002) 495–499.

[12] S. Zarska, D. Kulawik, J. Drabowicz, W. Ciesielski, A review of procedures of purification and chemical modification of carbon nanotubes with bromine, Fuller. Nanotubes, Carbon Nanostruct. 25 (2017) 563–569.

[13] Z. Chen, X. Du, M.–H. Du, C.D. Rancken, H.–P. Cheng, A.G. Rinzler, Bulk separative enrichment in metallic or semiconducting single–walled carbon nanotubes, Nano Lett. 3 (2003) 1245–1249.

[14] D. Hines, M.H. Rümmeli, D. Adebimpe, D.L. Akins, High–yield photolytic generation of brominated single–walled carbon nanotubes and their application for gas sensing, Chem. Comm. 50 (2014) 11568–11571.

[15] J. Li, L. Vaisman, G. Marom, J.–K. Kim, Br treated graphite nanoplatelets for improved electrical conductivity of polymer composites, Carbon 45 (2007) 744–750.

[16] I. Mazov, D. Krasnikov, A. Stadnichenko, V. Kuznetsov, A. Romanenko, O. Anikeeva, E. Tkachev, Direct vapor–phase bromination of multiwall carbon nanotubes, J. Nanotechnol. (2012) 954084.

[17] A.I. Romanenko, O.B. Anikeeva, A.V. Okotrub, L.G. Bulusheva, N.F. Yudanov, C. Dong, Y. Ni, Transport and magnetic properties of multiwall carbon nanotubes before and after bromination, Phys. Solid State 44 (2002) 659–662.

[18] E. Papirer, R. Lacroix, J.–B. Donnet, G. Nanse, P. Fioux, XPS study of the halogenation of carbon black – Part 1. Bromination, Carbon 32 (1994) 1341–1358.

[19] J.–F. Colomer, R. Marega, H. Traboulsi, M. Meneghetti, G. Van Tendeloo, D. Bonifazi, Microwave–assisted bromination of double–walled carbon nanotubes, Chem. Mater. 21 (2009) 4747–4749.

[20] L.G. Bulusheva, A.V. Okotrub, E. Flahaut, I.P. Asanov, P.N. Gevko, V.O. Koroteev, Yu.V. Fedoseeva, A. Yaya, C.P. Ewels, Bromination of double–walled carbon nanotubes, Chem. Mater. 24 (2012) 2708–2715.

[21] P.C. Eklund, N. Kambe, G. Dresselhaus, M.S. Dresselhaus, In–plane intercalate lattice modes in graphite–bromine using Raman spectroscopy, Phys. Rev. B 18 (1978) 7069–7079.

[22] A. Erbil, G. Dresselhaus, M.S. Dresselhaus, Raman scattering as a probe of structural phase transitions in the intercalated graphite–bromine system, Phys. Rev. B 25 (1982) 5451–5460.

[23] A.G. Souza Filho, M. Endo, H. Muramatsu, T. Hayashi, Y.A. Kim, E.B. Barros, N. Akuzawa, Ge.G. Samsonidze, R. Saito, M.S. Dresselhaus, Resonance Raman scattering studies in Br₂–adsorbed double–wall carbon nanotubes, Phys. Rev. B 73 (2006) 235413.

[24] G.M. do Nascimento, T. Hou, Y.A. Kim, H. Muramatsu, T. Hayashi, M. Endo, N. Akuzawa, M.S. Dresselhaus, Double–wall carbon nanotubes doped with different Br₂ doping levels: a resonance Raman study, Nano Lett. 8 (2008) 4168–4172.

[25] A.G. Souza Filho, V. Meunier, M. Terrones, B.G. Sumpter, E.B. Barros, F. Villalpando–Paez, J.M. Filho, Y.A. Kim, H. Muramatsu, T. Hayashi, M. Endo, M.S. Dresselhaus, Selective tuning of the electronic properties of coaxial nanocables through exohedral doping, Nano Lett. 7 (2007) 2383–2388.

[26] Y.K. Chen, M.L.H. Green, J.L. Griffin, J. Hammer, R.M. Lago, S.C. Tsang, Purification and opening of carbon nanotubes via bromination, Adv. Mater. 8 (1996) 1012–1015.

[27] E. Flahaut, R. Basca, A. Peigney, C. Laurent, Gram–scale CCVD synthesis of double–walled carbon nanotubes, Chem. Comm. (2003) 1442–1443.

[28] E.V. Lobiak, L.G. Bulusheva, E.O. Fedorovskaya, Y.V. Shubin, P.E. Plyusnin, P. Lonchambon, B.V. Senkovskiy, Z.R. Ismagilov, E. Flahaut, A.V. Okotrub, One–step chemical vapor deposition synthesis and supercapacitor performance of nitrogen–doped porous carbon–carbon nanotube hybrids, Beilstein J. Nanotechnol. 8 (2017) 2669–2679.

[29] Y. Zhao, D.G. Truhlar, Hybrid meta density theory methods for thermochemistry, thermochemical kinetics, and noncovalent interactions: the MPW1B95 and MPWB1K models and comparative assessments for hydrogen bonding and van der Waals interactions, J. Phys. Chem. A 108 (2004) 6908–6918.

[30] S. Grimme, J. Antony, S. Ehrlich, H. Krieg, A consistent and accurate ab initio parametrization of density functional dispersion correction (DFT–D) for 94 elements H–Pu, J. Chem. Phys. 132 (2010) 154104.

[31] A. Filipponi, P. D'Angelo, Accurate determination of molecular structures by x–ray absorption spectroscopy, J. Chem. Phys. 109 (1998) 5356–5362.

[32] E. Widenkvist, D.W. Boukhvalov, S. Rubino, S. Akhtar, J. Lu, R.A. Quinlan, M.I. Katsnelson, K. Leifer, H. Grennberg, U. Jansson, Mild sonochemical exfoliation of bromine–intercalated graphite: a new route towards graphene, J. Phys. D Appl. Phys. 42 (2009) 112003.

[33] L.G. Bulusheva, V.A. Tur, E.O. Fedorovskaya, I.P. Asanov, D. Pontiroli, M. Riccò, A.V. Okotrub, Structure and supercapacitor performance of graphene materials obtained from brominated and fluorinated graphites, Carbon 78 (2014) 137–146.

[34] K.L. Lu, R.M. Lago, Y.K. Chen, M.L.H. Green, P.J.F. Harris, S.C. Tsang, Mechanical damage of carbon nanotubes by ultrasound, Carbon 34 (1996) 814–816.

[35] M. Li, M. Boggs, T.P. Beebe, C.P. Huang, Oxidation of single–walled carbon nanotubes in dilute aqueous solutions by ozone as affected by ultrasound, Carbon 46 (2008) 466–475.

[36] D.–Q. Yang, J.–F. Rochette, E. Sacher, Functionalization of multiwalled carbon nanotubes by mild aqueous sonication, J. Phys. Chem. B 109 (2005) 7788–7794.

[37] R. Blume, D. Rosenthal, J.–P. Tessonnier, H. Li, A. Knop–Gericke, R. Schlögl, Characterizing graphitic carbon with X–ray photoelectron spectroscopy: a step––by–step approach, ChemCatChem 7 (2015) 2871–2881.

[38] U. Dettlaff–Weglikowska, V. Skákalová, R. Graupner, S.H. Jhang, B.H. Kim, H.J. Lee, L. Ley, Y.W. Park, S. Berber, D. Tománek, S. Roth, Effect of SOCl₂ treatment on electrical and mechanical properties of single–walled carbon nanotube network, J. Am. Chem. Soc. 127 (2005) 5125–5131.

[39] O.V. Sedelnikova, Yu.V. Fedoseeva, A.I. Romanenko, A.V. Gusel'nikov, O. Yu, Vilkov, E.A. Maksimovskiy, D.S. Bychanok, P.P. Kuzhir, L.G. Bulusheva, A.V. Okotrub, Effect of boron and nitrogen additives on structure and transport properties of arc–produced carbon, Carbon 143 (2019) 660–668.

[40] D.A. Bulushev, L.G. Bulusheva, S. Beloshapkin, T. O'Conner, A.V. Okotrub, K.M. Ryan, Pd clusters supported on amorphous, low–porosity carbon spheres for hydrogen production from formic acid, ACS Appl. Mater. Interfaces 7 (2015) 8719–8726.

[41] J. Zhong, L. Song, Z.–Y. Wu, S.–S. Xie, M. Abbas, K. Ibrahim, H. Qian, X–ray absorption near–edge structure and photoelectron spectroscopy of single–walled carbon nanotubes modified by a HBr solution, Carbon 44 (2006) 866–872.

[42] Yu.V. Fedoseeva, G.A. Pozdnyakov, A.V. Okotrub, M.A. Kanygin, Yu.V. Nastaushev, O.Y. Vilkov, L.G. Bulusheva, Effect of substrate temperature on the structure of amorphous oxygenated hydrocarbon films grown with a pulsed supersonic methane plasma flow, Appl. Surf. Sci. 385 (2016) 464–471.

[43] S. Kundu, Y. Wang, W. Xia, M. Muhler, Thermal stability and reducibility of oxygen–containing functional groups on multiwalled carbon nanotube surfaces, A quantitative high–resolution XPS and TPD/TPR study, J. Phys. Chem. C 112 (2008) 16869–16878.

[44] L.G. Bulusheva, A.V. Okotrub, I.P. Asanov, A. Fonseca, J.B. Nagy, Comparative study on the electronic structure of arc–Discharge and catalytic carbon nanotubes, J. Phys. Chem. B 105 (2001) 4853–4859.

[45] A. Yaya, C.P. Ewels, J.K. Efavi, B. Agyei–Tuffour, K. Kan–Dapaah, B. Onwona–Agyeman, E.K.K. Abavare, A. Hassanali, P.R. Briddon, A study of polybromide chain formation using carbon nanomaterials via density functional theory approach, Cogent Eng. 3 (2016) 1261509.

[46] P. Puech, A. Ghandour, A. Sapelkin, C. Tinguely, E. Flahaut, D.J. Dunstan, W. Bacsa, Raman G band in double–wall carbon nanotubes combining p doping and high pressure, Phys. Rev. B 78 (2008) 045413.

[47] G.M. do Nascimento, T. Hou, Y.A. Kim, H. Muramatsu, T. Hayashi, M. endo, N. Akuzawa, M.S. Dresselhaus, Comparison of the resonance Raman behavior of double–walled carbon nanotubes doped with bromine or iodine vapors, J. Phys. Chem. C 113 (2009) 3934–3938.

[48] A.L. Aguiar, E.B. Barros, V.P.S. Filho, H. Terrones, V. Meunier, D. Machon, Y.A. Kim, H. Muramatsu, M. Endo, F. Baudelet, A. San–miduel, A.G.S. Filho, Pressure tuning of bromine ionic states in double–walled carbon nanotubes, J. Phys. Chem. C 121 (2017) 10609–10619.

[49] O.V. Sedelnikova, C.P. Ewels, D.V. Pinakov, G.N. Chekhova, E. Flahaut, A.V. Okotrub, L.G. Bulusheva, Bromine polycondensation in pristine and fluorinated graphitic carbons, Nanoscale 11 (2019) 15298–15306.